Aquatic Toxicology 185 (2017) 171–182

Contents lists available at ScienceDirect

Aquatic Toxicology

journal homepage: www.elsevier.com/locate/aquatox

Endocrine and cellular stress effects of zinc oxide nanoparticles and nifedipine in marsh frogs *Pelophylax ridibundus*

Halina Falfushynska[a,b], Lesya Gnatyshyna[a,b], Oksana Horyn[b], Inna Sokolova[c], Oksana Stoliar[a,*]

[a] Research Laboratory of Comparative Biochemistry and Molecular Biology, Ternopil National Pedagogical University, Kryvonosa Str 2, 46027, Ternopil, Ukraine
[b] I.Ya. Horbachevsky Ternopil State Medical University, Maydan Voli, 1, 46001, Ternopil, Ukraine
[c] Marine Biology, Institute for Biological Sciences, University of Rostock, Albert-Einstein Str., 3, Rostock, Germany

ARTICLE INFO

Article history:
Received 31 August 2016
Received in revised form 2 December 2016
Accepted 7 February 2017
Available online 8 February 2017

Keywords:
Amphibians
Nano-zinc oxide
Pharmaceutical
Metallothionein
Endocrine system
Cytotoxicity

ABSTRACT

Freshwater organisms including amphibians experience increasing exposures to emerging pollutants such as nanoparticles and pharmaceuticals, which can affect their fitness and performance. We studied the effects of two common pollutants extensively used in industry, pharmaceutical and personal care products, nano-zinc oxide (nZnO) and a Ca-channel blocker nifedipine (Nfd), on endocrine status and cellular stress markers of the marsh frog *Pelophylax ridibundus*. Males were exposed for 14 days to nZnO (3.1 μM), Zn^{2+} (3.1 μM, as a positive control for nZnO exposures), Nfd (10 μM), and combination of nZnO and Nfd (nZnO + Nfd). Exposure to nZnO and Zn^{2+} led to an increase in Zn burdens, elevated concentrations of the metal-bound metallothioneins (MT-Me) in the liver and increased vitellogenin in the serum, whereas exposures to Nfd and nZnO + Nfd resulted in the metal release from MTs and a significant increase in the ratio of total to metal-bound MTs. This likely reflects oxidative stress caused by Nfd exposures as manifested in the elevated levels of oxyradical production, upregulation of superoxide dismutase activity (SOD) and increase in the total and oxidized glutathione concentrations in Nfd-exposed frogs. Zn-containing exposures upregulated activity of deiodinase (in nZnO and nZnO + Nfd exposures) and serum thyrotropin level (in the case of Zn^{2+}). All exposures caused an increase in DNA fragmentation, lipofuscin accumulation as well as upregulation of caspase-3 and CYP450 levels reflecting cytotoxicity of the studied compounds in the liver. Across all experimental treatments, nZnO exposures in the absence of Nfd had the least impact on the cellular stress traits or redox status in frogs. This indicates that at the low environmentally relevant levels of pollution, pharmaceuticals such as Nfd and free metals (such as Zn^{2+}) may represent a stronger threat to the health of the frogs than nZnO particles.

1. Introduction

In the past decades, the composition of pollutants in the surface waters have undergone a principal change as the chemical industrial pollution decreased and the environmental loads of complex, variable mixtures of pollutants from non-point municipal and agricultural wastes increased (Directive, 2013/39/EU; Burkart, 2007). Among the emerging pollutants, nanoparticles (Exbrayat et al., 2015) and pharmaceuticals (Schaider et al., 2016) are of particular concern due to their potentially high bioavailability and significant biological effects. These emerging pollutants also commonly co-occur in aquatic habitats thus presenting a potential for interaction. However, the effects of complex mixtures of pharmaceuticals and nanoparticles have not been well studied in aquatic organisms (Amin et al., 2014; Czech and Buda, 2015).

Nano zinc oxide (nZnO) are metal-based nanoparticles commonly used in electronics, personal care products (such as toothpaste, sunscreens and beauty products containing up to 20–25% of nZnO), and textiles to provide UV and antibacterial protection (Exbrayat et al., 2015). nZnO can enter surface waters from multiple non-point sources and accumulate in aquatic animals causing growing environmental and health concerns (Fabrega et al., 2012). The current level of nZnO in the surface waters of Europe is estimated at 100–500 ng/L in the industrial areas and predicted to increase in the future (NanoFATE 2010–2014; Dumont et al., 2015). nZnO can interact with pharmaceuticals and other organic pollutants enhancing degradation of photosensitive compounds in the water (Tan et al., 2011) and thereby affecting the composition of the

* Corresponding author.
E-mail address: oksana.stolyar@gmail.com (O. Stoliar).

http://dx.doi.org/10.1016/j.aquatox.2017.02.009
0166-445X/

wastewaters (Schaider et al., 2016). nZnO may also modulate the biological effects and toxicity of pharmaceuticals in aquatic organisms such as shown for nifedipine-nZnO interactions in freshwater bivalves (Falfushynska et al., 2015b). A cardiac drug nifedipine (Nfd) is a common pharmaceutical pollutant in surface waters. It is a calcium uptake inhibitor widely used as a cheap antianginal and antihypertensive medicine (Heberer, 2002; Kolpin et al., 2002). Nfd and its metabolite (dehydronifedipine) were detected in the effluents of the municipal sewage treatment plants and surface waters (Heberer, 2002; Kolpin et al., 2002). In a large urbanized watershed of New York City, environmental Nfd concentrations exceeded 1 $\mu g\,L^{-1}$ (2.9 nM) (Benotti and Brownawell, 2007). Nfd is photosensitive, and thus co-occurrence of Nfd with photoactive substances such as nZnO may modulate toxicity of these pollutants and potentially diminish of the individual activity of each of these substances (Tan et al., 2011).

Amphibians are excellent bioindicators of aquatic pollution and ecosystem health due to susceptibility of all life stages to dermal absorption of water-borne toxicants (Hermes-Lima and Storey, 1998). To date, the biological effects of metal-containing nanoparticles on amphibians have not been extensively studied, especially in the context of co-exposures in a complex environmentally-relevant mixtures of pollutants (Nations et al., 2011; Bacchetta et al., 2012; Zhang et al., 2012; Bour et al., 2015; Exbrayat et al., 2015; Falfushynska et al., 2016). In such mixtures, both direct and indirect (i.e. mediated by the release of Zn), toxicity of Zn-containing nanoparticles may be modulated by the presence of other pollutants, including pharmaceuticals. Pharmaceuticals such as Nfd and other Ca-channel blockers up-regulate antioxidant responses in different species (Ray et al., 2012; Velena et al., 2016). Oxidative stress pathways are also commonly involved in toxicity of free ionic metals and metal-containing nanoparticles thereby creating a molecular basis for interactions with Nfd. Furthermore, Nfd may affect metal toxicity by modulating metal transport (e.g. via blocking the Ca2+ channels) as well as due to the indirect, off-target effects in the groups distantly related to the target organisms (such as amphibians). Therefore, a comprehensive assessment of potential targets for combined toxicity is needed to understand the mechanisms of Nfd-nanoparticles interactions and their health effects in amphibians.

The present study aims to determine the molecular and cellular mechanisms of combined toxicity of nZnO and Nfd and assess the potential for Zn release and accumulation during single and combined exposures to nZnO and Nfd in a common marsh frog *Pelophylax ridibundus*. Based on the earlier studies that showed a strong oxidative stress response to nZnO exposure modulated by Nfd in freshwater bivalves with the involvement of metallothionein (Falfushynska et al., 2015b) and the susceptibility of amphibians to the endocrine-disrupting effects of environmental pollutants (Venturino et al., 2003; Hayes et al., 2006; Kloas et al., 2009; Falfushynska et al., 2016), we focused on the assessment of the parameters of Zn homeostasis (including the total Zn burdens and Zn binding to metallothioneins) as well redox and endocrine markers in frogs exposed to nZnO, Nfd and their mixtures. The oxidative stress response was evaluated from activity of a key antioxidant enzyme superoxide dismutase (SOD), the rates of oxyradical formation and levels of reduced and oxidized glutathione (GSH & GSSG). Oxidative lesions to membranes were determined by accumulation of the end-products of lipid peroxidation, malondialdehyde (assessed as the total concentration of the thiobarbituric acid-reactive substances, TBARS) and lipofuscin. Potential endocrine disruption due to nZnO and Nfd exposures was assessed by markers of thyroid function, levels of vitellogenin (Vtg) that serves as a Zn-carrier and a marker for xenoestrogen exposure, and cortisol as a general stress marker. Cytotoxicity was determined as the levels of hepatic cytochrome P450 oxidase (CYP450), DNA damage and activity of the apoptotic proteases caspase-3 and cathepsin D. This comprehensive assessment of biomarkers provides insights into the integrated cellular, molecular and endocrine responses of frogs to single and combined exposures to environmentally relevant levels of a common nanoparticle (nZnO) and pharmaceutical pollutant (Nfd) and the underlying toxicity mechanisms.

2. Materials and methods

2.1. Chemicals

5,5′-dithio-bis(2-nitrobenzoic acid) (DTNB), thiobarbituric acid (TBA), reduced glutathione (GSH), glutathione reductase from baker's yeast (*S. cerevisiae*), 2-vinylpyridine, quinine sulphate, dihydrorhodamine, salmon sperm DNA, Hoechst 33342, nitroblue tetrazolium (NBT), acetyl-Asp-Glu-Val-Asp *p*-nitroanilide, hemoglobin, serum albumin, phenazine methosulfate, phenylmethylsulfonyl fluoride (PMSF), chymotrypsinogen, cytochrome c, myoglobin, ubiquitin, insulin chain B oxidized, Sephadex G-50, β-mercaptoethanol, β-nicotinamide adenine dinucleotide oxidized (NAD^+), β-nicotinamide adenine dinucleotide phosphate reduced (NADPH), ethylenediaminetetraacetic acid (EDTA), and Triton *X-100* were purchased from Sigma (St. Louis, USA). nZnO particles (mean size 35 nm) were obtained from Sigma Chemical Company (St. Louis, USA). All other chemicals were obtained from the Synbias (Kyiv, Ukraine), Bayer (Kyiv, Ukraine) and Balkanpharma-Dupnitsa (Dupnitsa, Bulgaria) commercial suppliers. All reagents were of the analytical grade or higher.

2.2. Experimental exposures

The experiments were carried out in mid-September of 2013. Adult non-breeding males of marsh frog *Pelophylax ridibundus* (8–10 cm long) were collected from a pristine site in the upstream portion of river Seret (49°49′ N, 25°23′ E). Collections and experiments were performed in accordance with the national and institutional guidelines for the protection of animal welfare with permission of the Ministry of Ecology and Natural Resources of Ukraine, No 466/17.04.2013 and approval of the Committee on the Bio-Ethics at Ternopil National Pedagogical University (No 2/10.06.2013).

Frogs were transported to the laboratory in 60 L cages with aerated native water. The preliminary acclimation and experimental exposures were carried out in 40 L tanks filled with aerated, softened tap water. After seven days of preliminary acclimation, frogs were randomly distributed into five groups (15 individuals per group) and exposed for 14 days to one of the following conditions: 1) control (C), 2) nZnO (corresponding to 3.1 μM Zn), 3) Nfd (10 μM), 4) combination of nZnO (3.1 μM) and Nfd (10 μM), or 5) Zn^{2+} (added as $ZnSO_4$, 3.1 μM) as a positive control for Zn effects. A static renewal design was used, with water changed and chemicals replenished every two days. Throughout the experiment, the frogs were fed with commercial sticks "Turtle menu" (21% of protein, Aquarius, Ukraine). These conditions of exposures were the same as used in an earlier study on bivalve mollusks and reflected the lowest observed effect concentrations in the study of mollusk (Falfushynska et al., 2015b). The utilized concentrations were the same as for the studied early mollusks that reflected the lowest observed effect concentrations in the study of mollusks (Falfushynska et al., 2015b). To the best of our knowledge, we don't know about other studies of the effect of waterborne Nfd on the aquatic animals. So we selected the biologically active concentration basing on the previous results (Falfushynska et al., 2015b) and on the range of concentrations in the studies with human cell cultures (from 100 nM to 100 μM) (Hinkle et al., 1987;

Kondo et al., 1995; Ding and Vaziri, 2000; Ludwiczek et al., 2007) and the plasma level of Nfd in the treated patients with preterm labor (≈130 ng/mL) (Papatsonis et al., 2007). The water quality parameters were periodically measured during the preliminary acclimation and experimental exposures and were: temperature 17 ± 1 °C, pH 7.3 ± 0.2, $CaCO_3$ 86.8 ± 1.0 mg L^{-1}, dissolved oxygen concentration 8.67 ± 0.51 mg L^{-1}, ammonia (NH_3/NH_4^+) and nitrite concentrations below 0.1 mg L^{-1}. There was no mortality of frogs during the experiments.

After exposures, the frogs were anesthetized by clove oil (Goulet et al., 2010). The heparinized blood was collected from the heart, and plasma was immediately separated by centrifugation at 10,000 × *g* for 10 min. For serum preparation, whole blood was allowed to clot and centrifuged for 10 min at 1500 × *g* for 10 min. PMSF (0.1 mM) was added to plasma/serum to inhibit proteolysis. The frogs were killed by a blow to the head, the spinal cord severed, and liver was immediately removed for experiments. Samples of perfused hepatic tissue, blood plasma or serum from 8 specimens in each group were prepared individually and kept at −20 °C (for three days or less) until analyses. Hepatic tissue was homogenized (1:10 w:v) at 4 °C in 0.1 M pH 7.4 phosphate buffer containing 100 mM KCl, 1 mM EDTA and 0.1 mM PMSF. The homogenate was centrifuged at 6,000 × *g* for 10 min at 4 °C. Protein concentration in the supernatant and blood plasma/serum was measured according to Lowry et al. (1951) with bovine serum albumin as a standard. Vitellogenin was determined in blood plasma, TSH and cortisol were determined in the blood serum, and all other biomarkers were measured in liver homogenates. The absorbance was measured with a UV/Vis spectrophotometer "LOMO-56" (LOMO, Russian Federation), and the fluorescence was measured on the f-max fluorescence microplate reader (Molecular Devices, USA).

2.3. Isolation and quantification of metallothioneins (MTs)

MTs were isolated from the liver homogenates as the thermostable proteins by size-exclusion chromatography on Sephadex G-50 (Suzuki, 1991). For each biological replicate, tissues from five individuals from each experimental group were pooled (70 mg of tissue per individual to the total of 350 mg).To obtain the initial thermostable protein extract, a 5% liver homogenate (w/v) was prepared in ice-cold 10 mM Tris-HCl buffer, pH 8.0, containing 10 mM 2-mercaptoethanol and 0.1 mM PMSF and centrifuged at 10 000 × *g* for 45 min at 4 °C. The supernatant was incubated under the 85 °C for 5 min and subsequently centrifuged at 10 000 × *g* for 45 min at 4 °C to precipitate heat-labile proteins. The supernatant of the second centrifugation containing metallothioneins was used for the size-exclusion chromatography. Fractions of the chromatographic peak with high absorbance at 254 nm and high D_{254}/D_{280} density ratio were identified as MT-containing peaks (Kagi and Schaffer, 1988), pooled to obtain the total sample volume of 10 mL and used for metal determination. The concentration of metal-containing metallothioneins (MT-Me) was calculated from the concentrations of metals in the MTs assuming that one molecule of MTs binds seven Zn^{2+} or Cd^{2+} ions or twelve Cu^{+} ions (Nielson and Winge, 1985). MT-Me values were expressed as μg g^{-1} FW.

Total concentration of MTs was assessed by the concentration of thiols using DTNB reduction method (Viarengo et al., 1997) after the ethanol/chloroform extraction of the liver tissue. The levels of MT were calculated assuming the relationship: 1 mol MTs = 20 mol GSH and expressed as μg of MTs per g of wet tissue mass (FW).

2.4. Metal determination

Zinc (Zn) levels in the liver tissues and Zn, copper (Cu), and cadmium (Cd) in metallothioneins were measured by atomic absorption spectroscopy. Briefly, 250 mg of fresh liver tissue or 10 mL of the pooled eluate of MTs fraction were digested in 5 mL 70% HNO_3 (Merck) for 3 h at 105 °C using air-tight acid-cleaned Teflon bomb. Concentration of Zn and Cu was analyzed by the atomic absorption spectrometer with flame detector (C-115, "LOMO", Russian Federation) and Cd was analyzed by the graphite furnace atomic absorption spectrometer S-600 ("Selmi", Ukraine). The detection limits for metals were 0.1 μg g^{-1} wet mass (WM) for tissue and 1 μg L^{-1} for tap water. The reliability of the metals measurements was assessed by analyzing *ERM-CE 278* certified reference material (IRMM, Geel, Belgium); recovery of measurements was between 90% and 110%. Quality control was performed using Quality Control Sample for trace metal and method of Standard Addition (Beukelman and Lord, 1960). Metal concentrations in the tissues and MTs are presented as μg g^{-1} WM and nmol g^{-1} WM.

2.5. Oxidative stress biomarkers

Superoxide dismutase (SOD, EC 1.15.1.1) activity was measured at 25 °C as described in Beauchamp and Fridovich (1971) following the rate of the inhibition of superoxide-dependent aerobic reduction of NBT at 535 nm. SOD activity was expressed as units mg^{-1} soluble protein, assuming that 1 U of SOD activity inhibits the rate of NBT reduction by 50%.

Total glutathione concentration (μmol g^{-1} WM) was quantified by the glutathione reductase recycling assay calibrated with reduced glutathione (GSH) as a standard (Anderson, 1985). To estimate the oxidized glutathione (GSSG) level, the protein free sample was treated with 2% 2-vinylpyridine prior to the glutathione reductase recycling assay (Griffith, 1980). The rate of 5-thionitrobenzoic acid formation was monitored spectrophotometrically at 412 nm. The redox–index of glutathione (RI GSH) was calculated as the ratio of concentrations of reduced to total glutathione.

The rates of formation of oxyradicals (OxyR) in liver homogenates were determined at 25 °C using an ROS-sensitive dye dihydrorhodamine converted by reactive oxygen species (ROS) to the fluorescent rhodamine-123 (Viarengo et al., 1999). Fluorescence signal was detected by *f*-max fluorescence plate-reader [excitation = 485 nm, emission = 538 nm] at time 0 and after 20 min, and the rates of oxyradicals formation were calculated from these two values.

Lipid peroxidation (LPO) was determined in the supernatant of the liver homogenate by the concentrations of thiobarbituric acid-reactive substances (TBARS) (Ohkawa et al., 1979). A molar extinction coefficient of $1.56 \cdot 10^5$ M^{-1} cm^{-1} was used. Lipofuscin concentration in liver tissue was determined using chloroform: methanol (2:1, v/v) extraction of the homogenate. The lower clear chloroform phase obtained after the centrifugation was dried and redissolved in chloroform. The fluorescent signal of lipofuscin was detected by using an *f*-max fluorescence plate-reader [excitation = 350 nm, emission = 450 nm]. A freshly prepared solution of quinine sulphate (1 μg mL^{-1} of 0.1N H_2SO_4) was used as a standard (Manibabu and Patnaik, 1997; Falfushynska et al., 2015a).

2.6. Endocrine markers

A semi-quantitative Biomarker ELISA Kit (Biosense, Norway) was used to determine of vitellogenin (Vtg) concentration according to the manufacturer's protocol. Briefly, a dilution series of frog blood plasma was incubated in the microtiter plates overnight at 4 °C. Primary mouse monoclonal antibody against carp vitellogenin and secondary antibody conjugated with horseradish peroxidase were successively added to each microplate well and incubated. Free components were washed away, and the absorbance was measured at 492 nm in an ELISA reader (Awareness Technology Stat-Fax-303+ Microstrip Reader, USA).

The blood serum thyrotropin (TSH) and cortisol concentrations were measured with diagnostic ELISA kits using biotin-streptavidin-ELISA detection system and the 96-well-plate solid phase competitive ELISA Kit, respectively (Sigma-Aldrich, USA) according to the manufacturer's instructions. The absorbance was measured at 450 nm in an ELISA reader (Awareness Technology Stat-Fax–303 + Microstrip Reader, USA).

Hepatic deiodinase (EC 1.97.1.10) activity was detected in the microsomal pellet of the liver using tetraiodothyronine (T_4) as a substrate (Frankenfeld et al., 2002; Falfushynska et al., 2016). Microsomal pellet was obtained by calcium (80 mM $CaCl_2$) precipitation of the postmitochondrial supernatant of liver tissue in 10 mM Tris-HCl buffer, pH 7.4 (Cinti et al., 1972). The deiodinase assay contained 100 μL of the microsomal pellet (Cinti et al., 1972) and 2 μM T_4 in a final volume of 125 μL, and was incubated at 37 °C for 60 min. The reaction was stopped by the addition of 250 μL ice-cold 96% ethanol. The amount of formed triiodothyronine was determined in the ethanol extracts using an ELISA kit (Sigma Aldrich, USA). The deiodinase activity was expressed as nmol T_3 g^{-1} WM.

For all ELISA assays, linearity was tested using serial dilutions of the samples and compared to the dilutions of the respective standards provided with the kits. Samples showed acceptable linearity with an average R^2 of 0.97 ± 0.02 and the lines that were parallel to the standard curve.

2.7. Cytotoxicity assays

DNA damage in the liver was evaluated by the levels of protein-free DNA strand breaks by the alkaline DNA precipitation assay (Olive, 1988; Falfushynska et al., 2015a) using Hoechst 33342 dye. To reduce the possible interference with traces of sodium dodecyl sulphate (SDS), the assay was conducted in the presence of 0.4 M NaCl, 4 mM sodium cholate, and 0.1 M Tris (pH 9) (Bester et al., 1994). Fluorescence signal was detected by *f*-max fluorescence plate-reader (excitation = 360 nm, emission = 450 nm).

Activity of an executor caspase-3 (a marker of apoptosis) was assayed colorimetrically based on the hydrolysis of peptide acetyl-Asp-Glu-Val-Asp *p*-nitroanilide (Ac-DEVD-pNA) that produces a colored product *p*-nitroaniline (pNA) detected at 405 nm (ε = 10.5 mM^{-1} cm^{-1}) (Bonomini et al., 2004; Falfushynska et al., 2015a).

Cathepsin D (EC 3.4.23.5) activity was determined at 280 nm using 1% acid-denatured hemoglobin as a substrate as described by Dingle et al. (1971). Free cathepsin D activity was assessed in tissue homogenate without detergent addition, whereas the total cathepsin D activity was measured after Triton X100 treatment. Lysosomal cathepsin D activity was calculated as a difference of total and free activities. Activities were determined using a standard curve with thyrosine, and expressed as nmol tyrosine min^{-1} mg^{-1} of soluble extracted protein.

Cytochrome P450 (CYP450) concentration was measured in the microsomal pellet of the liver using the semi-quantitative Biomarker ELISA Kit (Biosense, Norway) according to the manufacturer's protocol. Absorbance was detected at 492 nm in an ELISA reader (Awareness Technology Stat-Fax-303+ Microstrip Reader, USA).

2.8. Statistical analysis

For analysis of MT-Me, sample size was 3 per group, each biological replicate consisting of the pooled tissues from five frogs. For all other traits and experimental treatment groups, sample size was 8. The data are presented as means ± standard deviation (SD) unless indicated otherwise. Data were tested for normality and homogeneity of variance by using Kolmogorov-Smirnoff and Levene's tests, respectively. Whenever possible, data were normalized by Box-Cox common transforming method. One-way ANOVA was used to test the effect of experimental exposures, followed by post hoc procedures. For the data that were not normally distributed, non-parametric tests (Kruskall–Wallis ANOVA and Mann–Whitney *U* test) were performed.

Normalized, Box-Cox transformed data were subjected to the principal component analysis (PCA) to differentiate individual specimens by the set of the biomarkers. Pearson's test was used to assess correlations between the studied traits. The classification tree based on all studied traits was built using Classification and Regression Tree (CART) software using raw (non-transformed) data. CART analysis presents a snapshot of the complex relationships of the variables in the data set and can be used in constructing an informative model of important associations. A classification tree splits the data based on similarity filtering out the "noise" and identifying the most important biomarker for each group (Breiman et al., 1984). All statistical calculations were performed with Statistica v. 12.0 and Excel for Windows-2013. Differences were considered significant if the probability of Type I error was less than 0.05.

3. Results

3.1. Zinc accumulation and metallothionein levels

Exposure of frogs to Zn^{2+} or nZnO led to substantial accumulation of Zn in the liver (Fig. 1A). Co-exposure to Nfd did not affect Zn accumulation during nZnO exposure (Fig. 1A). All experimental exposures led to an increase in the total levels of MTs (MT-SH), which were the highest in Zn^{2+} and Nfd-exposed groups (172 and 190% of control, respectively) (Fig. 2B). Notably, the amount of MT bound to metals was elevated in nZnO and Zn^{2+}- exposed frogs but significantly suppressed in their Nfd-exposed counterparts, compared to the control (Fig. 1C). Zn was the main metal bound to MTs in all exposures (~80% in their metal molar composition in all groups with Cd and Cu accounting for ~20%, data not shown). Suppression of the metal binding resulted in the significantly higher ratios of the total to metal-bound MTs in Nfd and Nfd-nZnO groups (by ~4.0- and 2.6- fold, respectively) (Fig. 1D). In contrast, the ratio of the total to metal-bound MTs in Zn^{2+} and nZnO-exposed frogs remained at the control levels reflecting the concomitant increase in the total MT-SH and metal-bound MT-Me (Fig. 1B–D).

3.2. Oxidative stress response

Exposure to Nfd alone caused a strong oxidative stress response indicated by a considerable increase in the rate of ROS generation (by 1.6-fold) and increase in the SOD (~2.4-fold), GSH (~6.1-fold) and GSSG (~2.5-fold) levels (Fig. 2A–D). No accumulation of lipid oxidative lesions (indicated by TBARS or lipofuscin levels) was found in Nfd-exposed animals (Fig. 2E, F). Exposure to nZnO in combination with Nfd partially counteracted the pro-oxidant effects of Nfd (Fig. 2). Exposure to ionic Zn^{2+} led to the suppression of the ROS formation rates, an increase in SOD activity and a slight but significant increase in the concentrations of GSSG and lipofuscin. Similar to Zn^{2+}, exposure to nZnO led to a suppression of ROS formation, and increase in GSSG and lipofuscin levels but the magnitude of changes was smaller than in the case of Zn^{2+} exposure (Fig. 2).

3.3. Endocrine markers

Serum thyrotropin level was significantly elevated by Zn^{2+} exposure (~2.1-fold) and slightly but significantly (by 18%) in nZnO and Nfd co-exposure (Fig. 3A). Deiodinase activity in the liver was up-regulated by nZnO and nZnO + Nfd exposures but not by Zn^{2+} or Nfd alone (Fig. 3B). Exposure to nZnO and Zn^{2+} led to increase

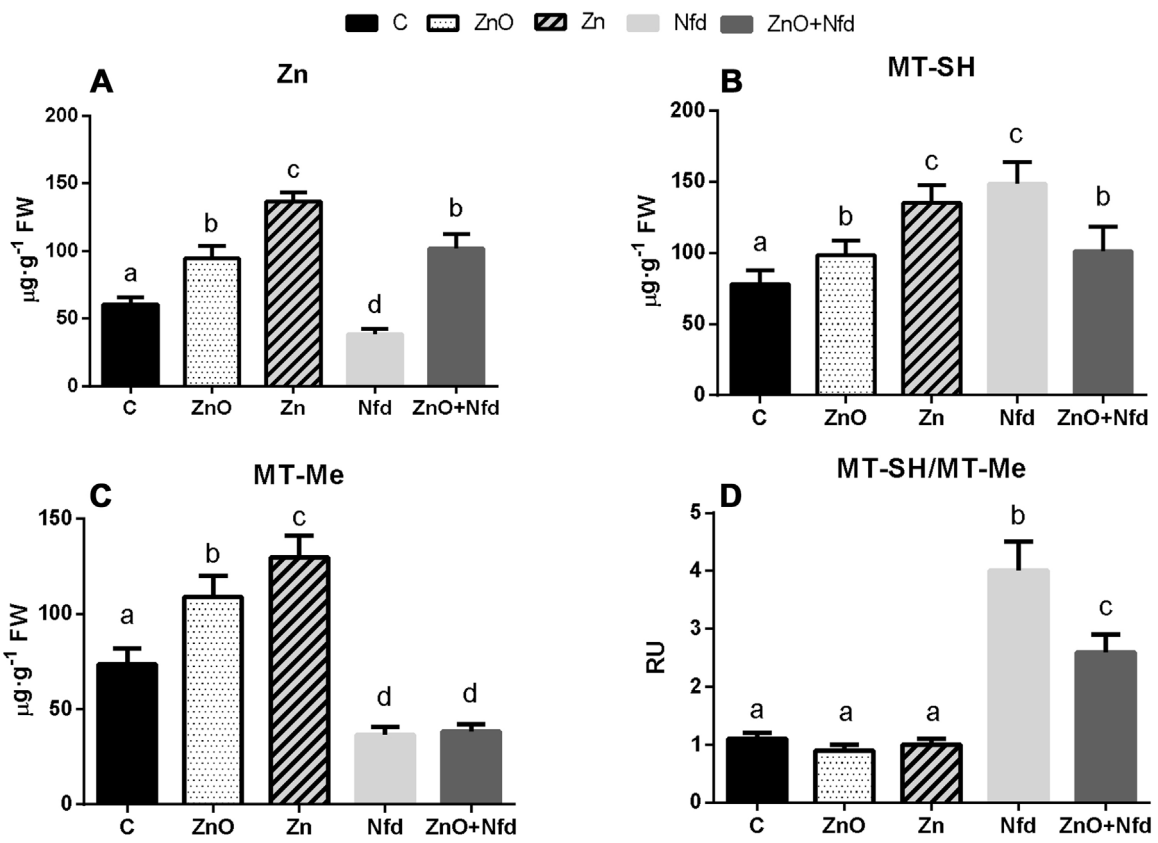

Fig. 1. Effects of experimental exposures to nanoform of ZnO (nZnO), zinc (Zn), nifedipin (Nfd) and the combination of nZnO + Nfd on tissue levels of Zn (A), metallothionein total (MT-SH) (B) and metalated (MT-Me) (C) concentrations and the ratio of the concentrations of MT-SH/MT-Me in the liver of frog *P. ridibundus*. Data are presented as means ± SD. N = 8 with the exception for metallothionein-bound Zn, where N = 3 (for pooled samples from 5 specimens each). Here and on Figs. 2–4, the columns that share the same letters indicate the values that are not significantly different ($p > 0.05$).

of vitellogenin level in the blood serum, whereas exposures to Nfd and nZnO + Nfd had the opposite effect (Fig. 3C). The level of cortisol was stable in most experimental groups except for a small decrease in the nZnO and Nfd co-exposure (Fig. 3D).

3.4. Cytoxicity markers

The CYP450 levels were up-regulated by all exposures, with the strongest increase in nZnO and nZnO + Nfd groups (Fig. 4A) attesting the activation of microsomal biotransformation in the liver. Occurrence of the DNA strand breaks increased in response to all experimental exposures, especially strongly in Zn^{2+}-exposed group (Fig. 4B). Caspase-3 activity was also stimulated by all experimental exposures with the strongest increase in nZnO + Nfd group followed by Zn^{2+}-exposed group (Fig. 4C). Total and free cathepsin activity was suppressed by nZnO and upregulated by all other experimental exposures (Fig. 4D).

3.5. Data integration

Principal component analysis showed that 65% of variation in the studied traits was explained by the first two principal components (Factors 1 and 2) (Fig. 5A). Nfd-exposed groups were clearly separated along the first principal component. The first principal component explained 38% of the total variation and had high loadings (≥0.6) of oxidative stress markers in the liver (SOD, GSH, GSSG, OxyR), as well as MT-Me, Zn-MT and Zn level in the liver and vitellogenin in blood plasma. Control group separated along the second principal component (27% of variation). The second principal component had high loadings (≥0.6) of SOD, MT-SH, caspase 3, cathepsin D both free and total activity in the liver, as well as thyrotropin in blood serum. Zn-exposed groups (including those exposed to Zn^{2+} or nZnO alone) had similar loadings on Factor 1 and 2 opposite to the loadings of the two Nfd-exposed groups.

Pearson correlation analysis revealed multiple associations between most studied indices (Supplement 1, Fig. 5B). Two association groups of traits where identified, within each the parameters were strongly and positively correlated with each other: 1) oxidative stress parameters including SOD, GSH, GSSG and MT-SH; 2) tissue levels of Zn, MT-Me and endocrine characteristics. Among these two groups, multiple negative correlations were observed. Vitellogenin had the highest number of correlations (seven positive correlations with other endocrine characteristics and the levels of MT-Me and Zn in the liver, and seven negative correlations with oxidative stress indices and MT-SH). Notably, levels of MT-SH did not correlate with MT-Me or Zn levels (Fig. 5B).

4. Discussion

4.1. Bioavailability and binding of Zn and its modulation by Nfd

Our data show that Zn from nZnO is bioavailable to the frogs *P. ridubundus* as indicated by Zn accumulation in the frog liver from all Zn-containing exposures (Zn2+, nZnO and nZn + Nfd) indicating that Zn from the nanoparticles is bioavailable to frogs. Furthermore, Zn was released from nZnO in the frog tissues as demonstrated by the elevation of MT-Me levels during nZnO exposures, comparable to that found in Zn^{2+}-exposed frogs. Tissue uptake of Zn from nZnO was also found in the intestine and liver of tilapia (*Oreochromis niloticus*) during exposures to high concentrations of nZnO (1 and

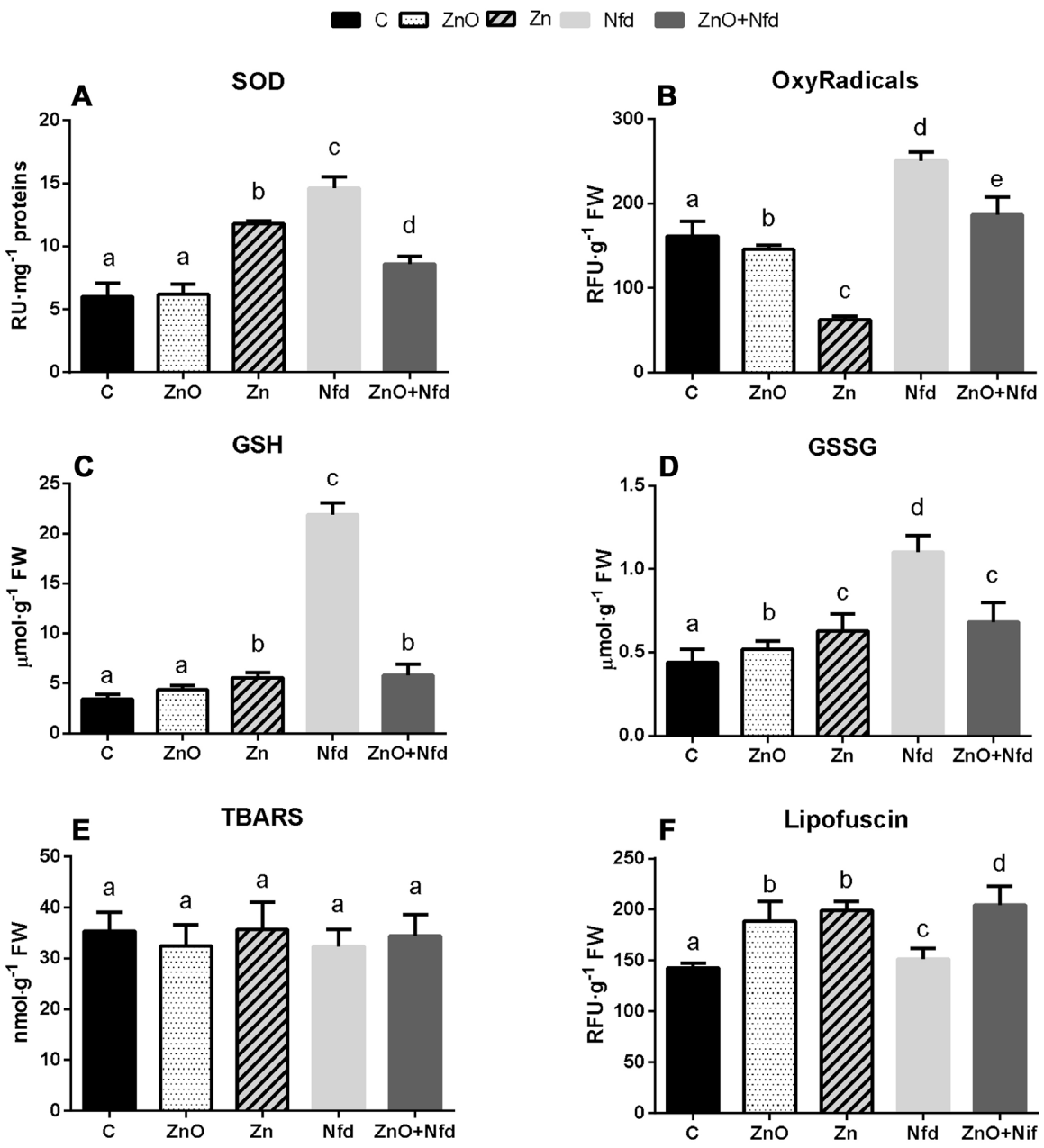

Fig. 2. Oxidative stress parameters in the liver of frog *P. ridibundus* exposed to nanoform of ZnO (nZnO), zinc (Zn), nifedipin (Nfd) and the combination of nZnO + Nfd. A, superoxide dismutase (SOD) activity; B, rate of oxyradical formation; C, reduced glutathione (GSH), D, oxidized glutathione (GSSG); E, TBARS concentration; F, lipofuscin concentration. Data are presented as means ± SD (N = 8).

10 mg L^{-1} corresponding to 15 and 150 µM Zn) for 14 days (Kaya et al., 2015). In contrast, freshwater bivalves *Unio tumidus* did not accumulate Zn during exposure to 3.1 µM nZnO (the same concentration as used in our present study); however, in the case of bivalves this may reflect the overall lower uptake and/or higher Zn excretion, because no Zn also accumulated in the bivalves exposed to 3.1 µM Zn^{2+} (Falfushynska et al., 2015b). Interestingly, during exposures to the nanoscale composite of Zn derived from an organic polymer vinylpirrolidone, Zn was not bioavailable to frogs and did not accumulate in the liver tissue or in the metal-bound MTs (Falfushynska et al., 2015a). This indicates that Zn bioavailability depends on the nature of the metal-containing particles including the chemical matrix in which Zn atoms are embedded.

A Ca-channel blocker Nfd had suppressive effect on the overall Zn levels in the control liver of *P. ridibundus* but not in those exposed to nZnO. In mammalian cells, Nfd affected uptake and accumulation of divalent metals including cadmium and iron by modulation of the divalent metal transporter-1 function (Hinkle et al., 1987; Leslie et al., 2006; Ludwiczek et al., 2007). In contrast, Nfd had no influence on Ca, Cd or Zn accumulation rates in the caddisfly *Hydropsyche sparna* (Poteat et al., 2012a,b). However, the participation of metallothioneins in these effects was not studied in the latter study. In the present study, exposure to Nfd strongly (by ~2-fold) suppressed the Zn-binding capacity of metallothioneins both in the positive control and nZnO + Nfd exposures. Nfd also has negative effects on the levels of vitellogenin (that acts as a Zn carrier) in frog, indicating a broad disturbance of homeostasis of this essential metal. Notably, a recent study in a freshwater bivalve *Unio tumidus* showed that, like in frogs, Nfd distorted the response to nZnO (Falfushynska et al., 2015a,b). However, Nfd caused elevation of MT-Me levels in nZnO-exposed bivalves, opposite to the effects seen in frogs (this study).

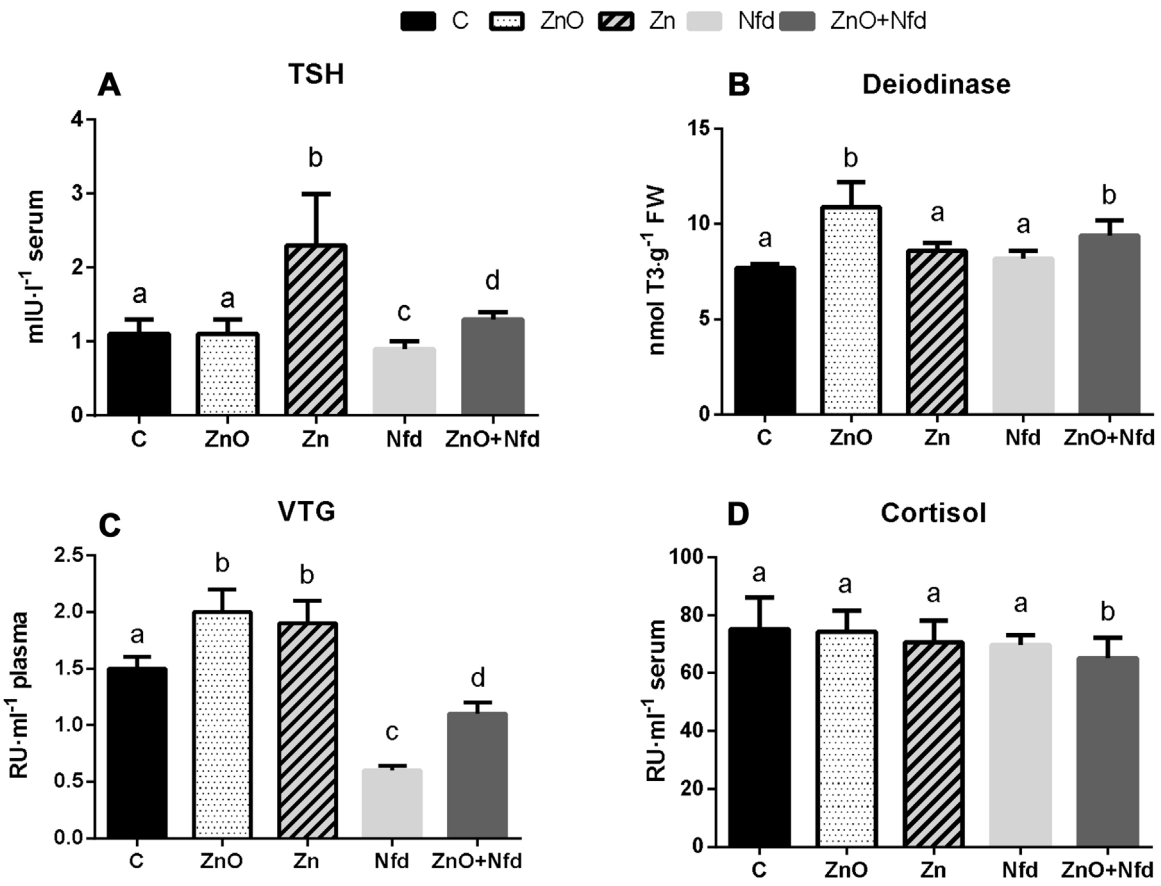

Fig. 3. Endocrine-related traits in frogs exposed to nanoform of ZnO (nZnO), zinc (Zn), nifedipin (Nfd) and the combination of nZnO + Nfd. A, thyrotropin concentration; B, Deiodinase activity; C, Vtg level; D, Cortisol concentration. Data are presented as means ± SD (N = 8).

These species-specific differences indicate that the direction and potentially the mechanisms of pollutant interactions (such as nZnO and Nfd) may differ between invertebrates and vertebrates.

A decrease in the proportion of the metal-bound MTs may reflect strong pro-oxidant effects of Nfd in frogs as shown by elevated ROS levels, an increase in oxidized glutathione (GSSG) and upregulation of antioxidants (SOD activity and GSH level). A concomitant increase in MT-SH and decrease in the metal-bound MTs (resulting in a strong upward shift of MT-SH/MT-Me ratio) indicates that a significant fraction of metallothionein in Nfd-exposed frogs was in the form of the partially or fully metal-free apo-protein. Metal-binding of metallothioneins is redox-sensitive so that oxidation of the thiol groups leads to a release of the bound metals and reduces the metal-binding capacity of the protein (Andersen et al., 1989; Kikuchi et al., 1990; Ngu and Stillman, 2009). Moreover, the metallothioneins of amphibians have particularly high protein heterogeneity and susceptibility to oxidative agents (Suzuki et al., 1986; Falfushynska et al., 2010, 2015a,b; Isani and Carpenè, 2014) making them prone to release metals (Falfushynska et al., 2010). Interestingly, in freshwater bivalves (*U. tumidus*) co-exposure to nZnO and Nfd led to the elevation of MT-Me levels (Falfushynska et al., 2015b), opposite to the effect observed in the frogs (this study). In bivalves an increase in Zn binding to MTs was associated with the reductive stress as indicated by elevated GSH levels and higher NADH/NAD ratio (Falfushynska et al., 2015b). This emphasizes a tight link between Zn binding to MTs and cellular redox status and may explain different redox-dependent effects of Nfd on the cellular Zn homeostasis in frogs and the bivalves.

4.2. Oxidative stress effects of nZnO, Zn^{2+} and Nfd exposures—similarity and differences

Exposure to ionic Zn^{2+}, nZnO, Nfd and/or their combination affected the redox status of the frog liver cells albeit the magnitude and the direction of the effects differed in different exposures. Exposure of frogs to nZnO and Zn^{2+} in the absence of Nfd suppressed ROS production and caused a modest increase of antioxidants and GSSG levels. Similarly, exposure of frogs to 1.3 μM of Zn- or Zn-contained nanoorganic particles for 14 days led to a strong decrease in ROS production (Falfushynska et al., 2016), in agreement with the well-established role of Zn as antioxidant (Valko et al., 2005). In freshwater bivalves, nZnO and Zn^{2+} exposures also led to activation of antioxidant defenses and a small but significant increase in ROS levels; however, this increase did not translate into the higher levels of oxidative lesions such as protein carbonyls or TBARS (Falfushynska et al., 2015b). Antioxidant effects of nZnO were also reported in broilers where dietary uptake of nZnO reduced TBARS levels and improved growth performance (Shoae-Hagh et al., 2014; Zhao et al., 2014). These findings contrast with the results of studies in laboratory mammals and mammalian cell lines that predominantly show oxidative effect of nZnO (Huang et al., 2010; Ali et al., 2012; Manke et al., 2013; Kaya et al., 2015; Yang et al., 2015). A dramatic increase in oxidative lesions and suppression of antioxidant activities was also reported for a freshwater snail *Limnaea luteola*; however, these effects were found at high, environmentally non-relevant concentrations of nZnO (32 mg L^{-1} corresponding to 395 μM Zn) (Ali et al., 2012). Overall, existing evidence indicates that in frogs (this study) and freshwater bivalves (Falfushynska

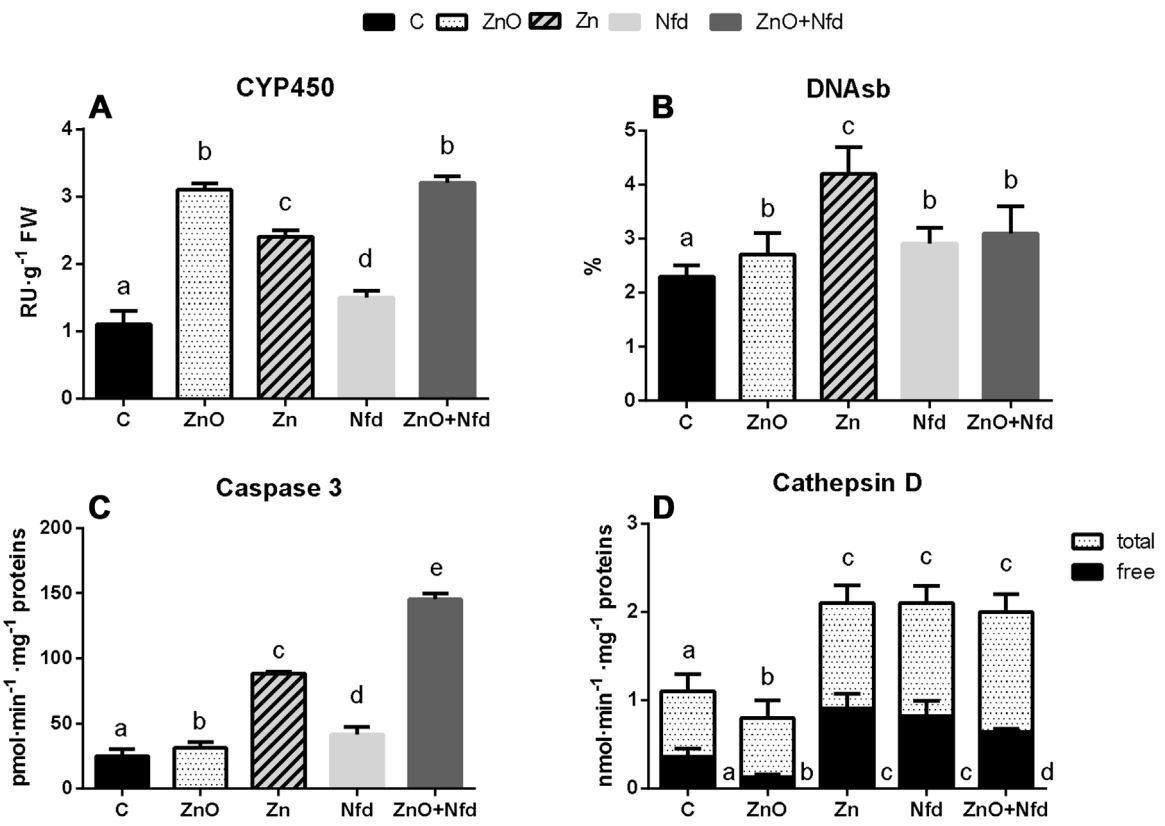

Fig. 4. Cytotoxicity markers in the liver of frog, exposed to nanoform of ZnO (nZnO), zinc (Zn), nifedipin (Nfd) and the combination of nZnO + Nfd. A, CYP-450 level; B, frequencies of the DNA strand breaks; C, caspase-3 activity; D, activities of the total and free cathepsin D. Data are presented as means ± SD (N = 8). The columns that share the same letters indicate the values that are not significantly different ($p > 0.05$).

et al., 2015b) environmentally relevant concentrations of nZnO do not induce oxidative stress and may under certain conditions act as antioxidants.

The strongest oxidative stress response (including upregulation of antioxidants SOD activity and GSH level and stimulation of ROS formation) in frogs was found during exposures to Nfd. Up-regulated levels of metallothionein and particularly its metal-unbound form in Nfd-exposed frogs also suggest that the thiol groups are involved in the antioxidant activity (Kang, 2006). These manifestations of oxidative stress are not accompanied by a strong signal of oxidative injury (as indicated by the near-background levels of TBARS and lipofuscin) (Fig. 2). This is similar to the Nfd effects in mammals where Nfd and other Ca-channel blockers suppress lipid peroxidation (Ray et al., 2012; Velena et al., 2016), reducing production of superoxide but increasing the NO levels (Wang et al., 2016). Similar to frogs, in freshwater bivalves *U. tumidus* Nfd exposure induced oxidative stress indicated by increased ROS production, lipid peroxidation and upregulation of SOD (Falfushynska et al., 2015b). The mechanisms of Nfd-induced modulation of the cellular redox balance in different organisms are not yet fully understood. In mice, Nfd exerts antioxidant effects via modulation of the iron transport by preventing iron overload via divalent metal transporter-1 and enhancing urinary iron excretion (Ludwiczek et al., 2007). Another possible mechanism for the antioxidant effects of Nfd described in mammals may include suppression of Ca^{2+}-dependent mitochondrial energy metabolism due to the blockage of Ca^{2+} entry and consequently, a decrease in the mitochondrial ROS production (De Marchi et al., 2014). These findings call for future in-depth mechanistic investigations of the effects of pharmaceuticals (including Nfd) in non-target species to fully understand the mechanisms of its strong effect on oxidative stress and distortions of Zn homeostasis in different distantly related species.

Notably, a co-exposure with nZnO alleviated the strong oxidative action of Nfd in frogs by suppressing ROS production and decreasing the degree of activation of SOD and GSH. There is no evidence for the strong interaction between Nfd and nZnO, and the effects of these chemicals on the redox parameters in frogs appear additive (Fig. 5A). Similar counterbalancing effects of Nfd and nZnO on redox traits were earlier found during co-exposures in freshwater bivalves *U. tumidus* (Falfushynska et al., 2015b). In human cell lines, oxidative effects of nZnO have been linked to the loss of membrane integrity resulting in Ca^{2+} influx, only partially alleviated by a Ca^{2+} channel blocker Nfd (Huang et al., 2010).

Our study also indicates a potentially strong involvement of metallothioneins in antioxidant defense of the frogs. Thus, exposure to Nfd stimulated expression of metallothioneins along with the activation of an enzymatic antioxidant SOD and upregulation of glutathione. Furthermore, a high ratio of MT-SH to MT-Me indicate that the excess metallothionein is not involved in the metal binding but rather contributes to other cellular functions, most likely ROS scavenging (Andersen et al., 1989; Kikuchi et al., 1990; Ngu and Stillman, 2009). This hypothesis is supported by significant positive correlations of antioxidant traits (such as SOD, GSH) with MT-SH levels in frogs. Similar correlated upregulation of metallothionein and SOD was observed in medaka *Oryzias melastigma* during exposure to bulk ZnO (~50 and 500 μM Zn), while in nZnO-exposed fish the oxidative stress response was absent (Wong et al., 2010).

4.3. Endocrine effects of Zn and nfd

Sensitivity of the endocrine system of frogs to environmental impacts is well documented (Venturino et al., 2003; Hayes

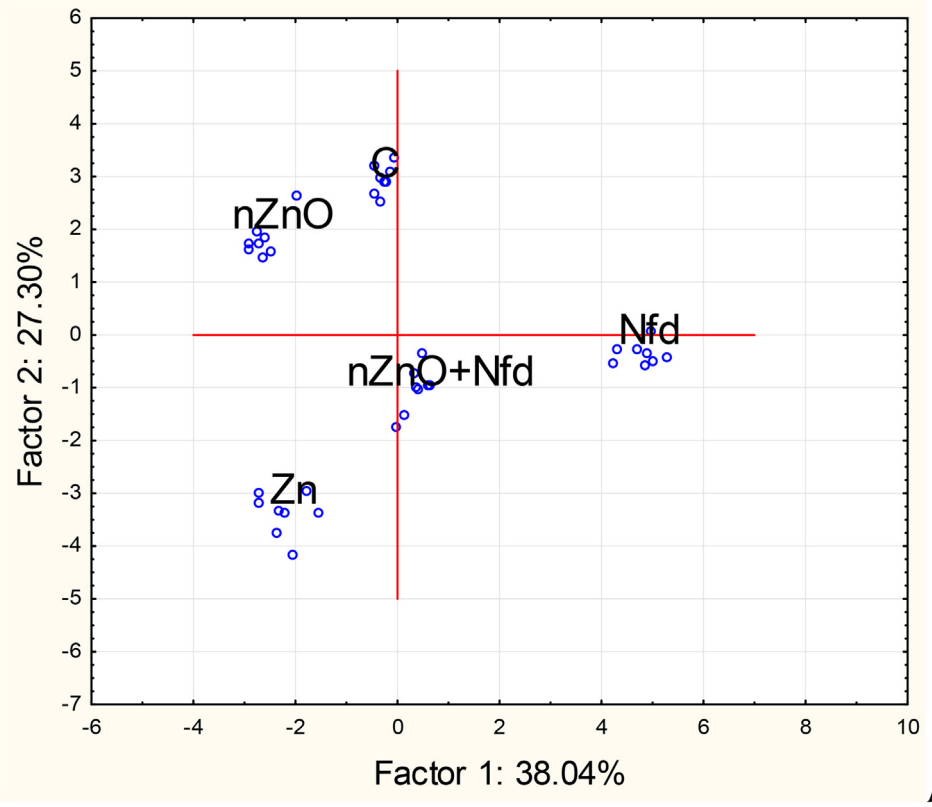

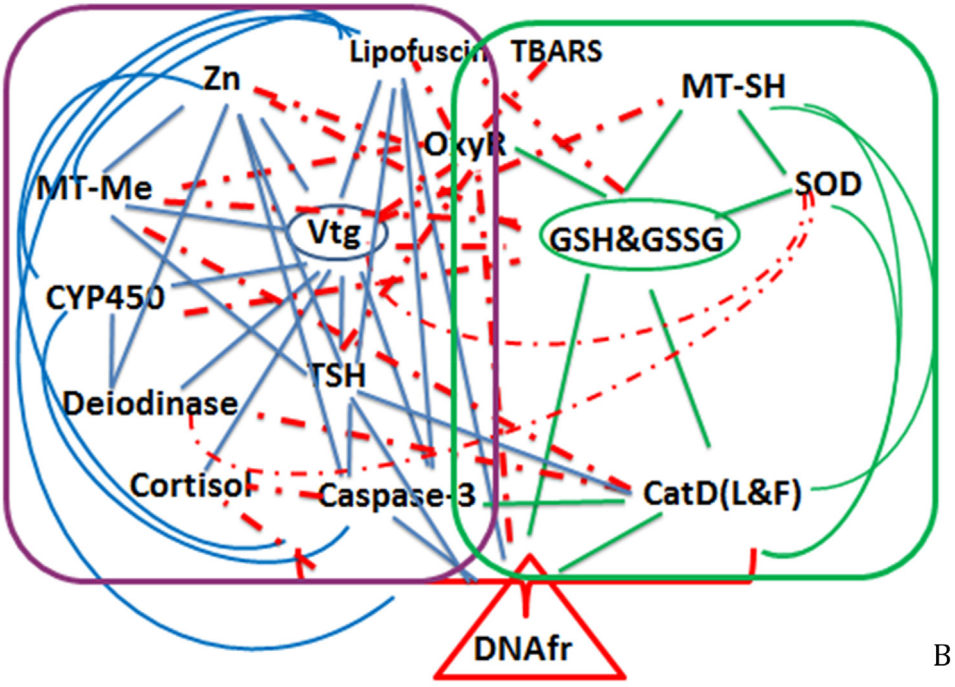

Fig. 5. Integrative analysis of the studied indices in *P. ridibundus* from different treatment groups.
A—results of the principal component analysis. Different symbols represent different treatment groups (C—control, nZnO-, Zn-, Nfd- and nZnO + Nfd-exposed).
B—a schematic representation of the relationships between the studied traits. Solid and dotted connector lines represent relationships with positive and negative correlations, respectively. Only significant correlations (based on Pearson correlation analysis, see Supplement) are shown. Abbreviations: MT-SH, total metallothionein concentration; MT-Me, metalated metallothionein concentration; TBARS, thiobarbituric acid-reactive substances concentration; GSH&GSH, glutathione reduced & oxidized concentrations; OxyR, oxyradical formation; Vtg, vitellogenin concentration; TSH, thyrotropin concentration; CatD(L&F), Cathepsin D (Lysosomal&Free) activities; DNAfr, DNA fragmentation. The scopes select the sets of positive correlations of MT-Me and MT-SH separately.

et al., 2006; Kloas et al., 2009; Hoffmann and Kloas, 2012) and is considered a major contributor to the dramatic decline of frog populations in the last decades (Rouhani Rankouhi et al., 2005; Whittaker et al., 2013). Most studies on environmental endocrine disruption have focused on the period of metamorphosis (Veldhoen et al., 2006), and less is known about the vulnerability of endocrine functions in adult amphibians. Our study indicates that thyroid and reproductive hormone functions of adult males of *P. ridibundus* are susceptible to the effects of the environmentally relevant concentrations of nZnO and Nfd, and these effects are linked with effects of exposures on Zn binding and homeostasis. Thus, levels of vitellogenin, an egg protein that serves as an index of xenoestrogen exposure in males (Palmer et al., 1998; Venturino et al., 2003; Rouhani Rankouhi et al., 2005), was upregulated during exposures to nZnO and Zn^{2+} and downregulated in Nfd exposures, in tight correlation with the changes in MT-Me levels (Pearson correlation coefficient $R = 0.91$, $p < 0.001$). Earlier, activation of vitellogenesis was shown in *P. ridibundus* males exposed for 14 days to 1.3 μM of Zn^{2+} or Zn-containing organic nanocomposite (Falfushynska et al., 2015a). Vitellogenin is a Zn transporter in the blood plasma supplying the Zn for the reproductive activity in oviparous vertebrates (Montorzi et al., 1995; Falchuk and Montorzi, 2001; Thompson et al., 2012). Therefore, upregulation of Vtg synthesis may contribute to the feminizing effects of nZnO and Zn^{2+} exposures. It is worth noting, however, that Vtg as a Zn-carrier protein may also affect other essential biological functions beyond oogenesis such as male and female gonad maturation, growth, cell proliferation and signaling, and ROS scavenging (MacDonald, 2000; Corona et al., 2007; Unuma et al., 2011; Thompson et al., 2012). In fish, Vtg was associated with immune defense via its effects on both recognizing pathogen-associated molecular patterns and promoting macrophage phagocytosis (Li et al., 2008). Therefore, Vtg upregulation in male frogs found in our study may reflect the involvement of this protein in other Zn-dependent biological processes rather than endocrine disruption.

Our study showed significant effects of nZnO, Zn^{2+} and Nfd exposures on thyroid-related traits (TSH and deiodinase activity), in agreement with the reported sensitivity of the amphibian thyroid system to environmental impacts (Kloas et al., 2009; Li et al., 2011). However, changes in TSH and deiodinase during experimental exposures were not coordinated. The deiodinase activity was mostly up-regulated by nZnO exposures, while TSH levels were stimulated by exposure to Zn^{2+}. Unlike frogs, Zn^{2+} exposures in rats suppressed deiodination activity in the liver; this effect was attributed to the inactivation of SH-groups in enzyme by Zn (González Pondal et al., 1995). In our present study, no evidence of the suppression of the thiol system (including MT-SH, GSH) was found in response to Zn^{2+} exposure in frogs which may explain the lack of Zn^{2+}-induced inhibition of deiodinase. In frogs, deiodinase activity positively correlated with Zn and Vtg levels as well as with CYP450 activity reflecting links of this enzyme to Zn supply and thyroid-dependent biotransformation activity in hepatic endoplasmic reticulum (Brown, 2005). The pituitary stimulation of thyroid activity (indicated by TSH levels) was also interrelated with Zn accumulation, MT-Me and Vtg levels in the frogs. However, this effect appeared to be concentration-dependent because 3.1 μM Zn^{2+} upregulated the TSH levels in the blood plasma of frogs (present study) while exposure to 1.3 μM Zn^{2+} suppressed it (Falfushynska et al., 2016).

The level of cortisol was not affected by the exposures to nZnO, Zn^{2+} or Nfd (except a slight decrease in nZnO + Nfd exposures). Similarly, no change in the serum cortisol levels was found in frogs exposed to Zn^{2+} or Zn-containing organic nanocomposites (Falfushynska et al., 2016). This may indicate that exposures to Zn^{2+}, Nfd or Zn-containing nanoparticles do not cause general stress in the frogs. Alternatively, this may reflect low contribution of cortisol to stress response in adult frogs which (unlike the larval stages) produce corticosterone as their primary glucocorticoid stress hormone (Narayan, 2013). Future studies using a broad screen of corticosteroid hormones would be needed to clarify the involvement of the general stress response in responses of adult amphibians to pharmaceuticals and Zn-containing nanoparticles.

4.4. Cytotoxicity of the exposures to nZnO and Nfd

All experimental exposures caused an increase in cytotoxicity markers including elevated levels of DNA fragmentation, upregulation of an apoptotic enzyme caspase 3, and lysosomal injury indicated by increased accumulation of lipofuscin and release of cathepsin D from lysosomes. Upregulation of CYP450 in the liver of exposed frogs (particularly in nZnO-related exposures) may indicate endoplasmic reticulum stress, similar to the effects shown during exposures to the high chronic doses of nZnO in mice (Yang et al., 2015). Nevertheless, among the experimental exposures, exposure to nZnO alone was the least cytotoxic. Notably, exposure to nZnO caused a decrease in the cathepsin D levels, whereas all other exposures prominently up-regulated the total and free cathepsin D activity.

Cytotoxicity of Zn^{2+} and Nfd has been previously described in other organisms. Zn is an important regulator of apoptosis in animals and at low concentrations can suppress apoptotic pathways and inhibit caspases (Truong-Tran et al., 2001), but induce apoptosis at high concentrations (Franklin and Costello, 2009). Earlier studied showed that Nfd induces apoptosis in human tumor cells (Kondo et al., 1995) and causes embryonic malformation in the clawed frog, *Xenopus laevis* (Boğa Pekmezekmek et al., 2015). Our study indicates that environmentally relevant level of Zn^{2+} (3.1 μM) fall into the apoptosis-inducing range of concentrations for *P. ridibundus*. Exposure to Nfd induced moderate cytotoxicity, which was observed in both single Nfd exposures and co-exposure to Nfd with nZnO. The major response involved stimulation of cathepsin D activity and release, and (in the case of the combined exposure), caspase-3 activation.

4.5. Conclusions and perspectives

Exposure to nZnO in the absence of other stressors caused minimal physiological and cytological disturbances in the frogs indicating that environmentally relevant concentrations of this pollutant alone are not a significant health concern for this species. This conclusion is also supported by the close proximity of the control and nZnO exposed groups in the plane of the two first principal components which integrate the studied physiological and molecular traits. This contrasts with earlier studies using acute exposures to high nZnO concentrations that showed high levels of oxidative injury in aquatic organisms (Wong et al., 2010; Gagné et al., 2013), as well as embryonic malformations and growth retardation in frogs (Nations et al., 2011). This discrepancy emphasizes the need for the long-term studies on the effects of environmentally relevant, low concentrations of metal-containing nanoparticles to reliably assess the associated environmental and health risks. The observed shifts in the endocrine status of nZnO exposed frogs emphasize the tight links between Zn homeostasis and the studied hormonal traits rather than nZnO-induced endocrine disruption. Combined exposure to a pharmaceutical Nfd did not result in the increase on nZnO toxicity; rather, the effects of the combined exposure in the selected conditions reflected the predominant signal from one of the compounds (i.e. metal release from MT by Nfd), or in some cases opposite effects of Nfd and nZnO (such as suppression of the Nfd-induced oxidative stress by nZnO). This illustrates the complexity of pollutant interactions in aquatic organisms that cannot be directly predicted from the effects of a single pollutant, and suggests that

at the present-day environmental levels of pollution, pharmaceuticals such as Nfd may represent a stronger threat to the amphibian health than nZnO particles.

Acknowledgements

This work has been supported by the Ministry of Education and Science of Ukraine (Projects # 125B; 131B), U.S. Civilian Research and Development Foundation (CRDF) Cooperative Grants Program award (UKB1-7109-TE-13) to O.B.S. and I.M.S., Fulbright Scholarship, Alexander von Humboldt Foundation and West-Ukrainian Biomedical Research Centre grant to H.F. The authors are grateful to Dr. O.V. Fedorova (I.Ya. Postovsky Institute of Organic Synthesis of Russian Academy of Science, Yekaterinburg, Russia) for the idea to study the ecotoxicity of waterborne Nfd.

References

Ali, D., Alarifi, S., Kumar, S., Ahamed, M., Siddiqui, M.A., 2012. Oxidative stress and genotoxic effect of zinc oxide nanoparticles in freshwater snail *Lymnaea luteola* L. Aquat. Toxicol. 124–125, 83–90, http://dx.doi.org/10.1007/s12011-014-0158-6.

Amin, M.T., Alazba, A.A., Manzoor, U., 2014. A review of removal of pollutants from water/wastewater using different types of nanomaterials. Adv. Mater. Sci. Eng., 24, http://dx.doi.org/10.1155/2014/825910, Article ID 825910.

Andersen, R.A., Daae, H.L., Mikalsen, A., Alexander, J., 1989. Occurrence of various forms of metallothionein in the rat after a short-term cadmium injection regimen. Comp. Biochem. Physiol. 93C, 367–375, http://dx.doi.org/10.1016/0742-8413(89)90249-1.

Anderson, M.E., 1985. Determination of glutathione and glutathione disulfide in biological samples. Meth. Enzymol. 113, 548–555.

Bacchetta, R., Santo, N., Fascio, U., Moschini, E., Freddi, S., Chirico, G., Camatini, M., Mantecca, P., 2012. Nano-sized CuO, TiO2 and ZnO affect xenopus laevis development. Nanotoxicology 6, 381–398, http://dx.doi.org/10.3109/17435390.2011.579634.

Beauchamp, C., Fridovich, I., 1971. Superoxide dismutase: improved assay and an assay applicable to acrylamide gels. Anal. Biochem. 44, 276–287.

Benotti, M.J., Brownawell, B.J., 2007. Distributions of pharmaceuticals in an urban estuary during both dry- and wet-weather conditions. Environ. Sci. Technol. 41, 5795–5802.

Bester, M.J., Potgieter, H.C., Vermaak, W.J., 1994. Cholate and pH reduce interference by sodium dodecyl sulfate in the determination of DNA with Hoechst. Anal. Biochem. 223, 299–305.

Beukelman, T.E., Lord, S.S., 1960. The standard addition technique in flame spectrometry. Appl. Spectrosc. 14, 12–17.

Boğa Pekmezekmek, A., Binokay, U.S., Seçilmiş, M.A., Kumcu, E., Şimşek, E., Akillioğlu, K., Sertdemir, Y., Özaykan, B., 2015. Evaluating the teratogenicity of ritodrine and nifedipine using a frog embryo teratogenesis assay (FETAX). Drug Chem. Toxicol. 38, 254–265, http://dx.doi.org/10.3109/01480545.2014.947423.

Bonomini, M., Dottori, S., Amoroso, A., Arduini, A., Sirolli, V., 2004. Increased platelet phosphatidylserine exposure and caspase activation in chronic uremia. J. Thromb. Haemost. 2, 1–8.

Bour, A., Mouchet, F., Verneuil, L., Evariste, L., Silvestre, J., Pinelli, E., Gauthier, L., 2015. Toxicity of CeO2 nanoparticles at different trophic levels-effects on diatoms, chironomids and amphibians. Chemosphere 120, 230–236, http://dx.doi.org/10.1016/j.chemosphere.2014.07.012.

Breiman, L., Friedman, J.H., Olshen, R.A., Stone, C.J., 1984. Classification and Regression Trees. Monterey, CA: Wadsworth & Brooks/Cole Advanced Books & Software.

Brown, D.D., 2005. The role of deiodinases in amphibian metamorphosis. Thyroid 15, 815–821, http://dx.doi.org/10.1089/thy.2005.15.815.

Burkart, M.R., 2007. Diffuse pollution from intensive agriculture: sustainability, challenges, and opportunities. Water Sci. Technol. 5, 17–23, http://dx.doi.org/10.2166/wst.2007.067.

Cinti, D.L., Moldeus, P., Schenkman, J.B., 1972. Kinetic parameters of drug metabolizing enzymes in Ca2+-sedimented microsomes from rat liver. Biochem. Pharmacol. 21, 3249–3256.

Corona, M., Velarde, R.A., Remolina, S., Moran-Lauter, A., Wang, Y., Hughes, K.A., Robinson, G.E., 2007. Vitellogenin, juvenile hormone, insulin signaling, and queen honey bee longevity. Proc. Natl. Acad. Sci. U. S. A. 104, 7128–7133, http://dx.doi.org/10.1073/pnas.0701909104.

Czech, B., Buda, W., 2015. Photocatalytic treatment of pharmaceutical wastewater using new multiwall-carbon nanotubes/TiO2/SiO2 nanocomposites. Environ. Res. 137, 176–184, http://dx.doi.org/10.1016/j.envres.2014.12.006.

De Marchi, U., Thevenet, J., Hermant, A., Dioum, E., Wiederkehr, A., 2014. Calcium co-regulates oxidative metabolism and ATP synthase-dependent respiration in pancreatic beta cells. J. Biol. Chem. 289, 9182–9194, http://dx.doi.org/10.1074/jbc.M113.513184.

Ding, Y., Vaziri, N.D., 2000. Nifedipine and diltiazem but not verapamil up-regulate endothelial nitric-oxide synthase expression. J. Pharmacol. Exp. Ther. 292, 606–609.

Dingle, J.T., Barrett, A.J., Weston, P.D., Cathepsin, D., 1971. Characteristics of immunoinhibition and the confirmation of a role in cartilage breakdown. Biochem. J. 123, 1–13.

Directive 2013/39/EU of the European Parliament and of the Council of 12 August 2013 amending Directives 2000/60/EC and 2008/105/EC as regards priority substances in the field of water policy http://eur-lex.europa.eu/legal-content/EN/ALL/?uri=CELEX%3A32013L0039.

Dumont, E., Johnson, A.C., Keller, V.D., Williams, R.J., 2015. Nano silver and nano zinc-oxide in surface waters—exposure estimation for Europe at high spatial and temporal resolution. Environ. Pollut. 196, 341–349, http://dx.doi.org/10.1016/j.envpol.2014.10.022.

Exbrayat, J.M., Elara, N., Moudilou, E.N., Lapied, E., 2015. Harmful effects of nanoparticles on animals. J. Nanotechnol., http://dx.doi.org/10.1155/2015/861092, Article ID 861092.

Fabrega, J., Tantra, R., Amer, A., Stolpe, B., Tomkins, J., Fry, T., Lead, J.R., Tyler, C.R., Galloway, T.S., 2012. Sequestration of zinc from zinc oxide nanoparticles and life cycle effects in the sediment dweller amphipod *Corophium volutator*. Environ. Sci. Technol. 46, 1128–1135.

Falchuk, K.H., Montorzi, M., 2001. Zinc physiology and biochemistry in oocytes and embryos. Biometals 14, 385–395.

Falfushynska, H.I., Romanchuk, L.D., Stoliar, O.B., 2010. Reactivity of metallothioneins in frog *Rana ridibunda* treated by copper and zinc ions. Ukr. Biochem. J. 82, 17–26.

Falfushynska, H., Gnatyshyna, L., Fedoruk, O., Mitina, N., Zaichenko, A., Stoliar, O., Stoika, R., 2015a. Hepatic metalothioneins in molecular responses to cobalt, zinc, and their nanoscale polymeric composites in frog *Rana ridibunda*. Comp. Biochem. Physiol., 172C–173C, http://dx.doi.org/10.1016/j.cbpc.2015.04.006, 45–56.

Falfushynska, H., Gnatyshyna, L., Yurchak, I., Sokolova, I., Stoliar, O., 2015b. The effects of zinc nanooxide on cellular stress responses of the freshwater mussels *Unio tumidus* are modulated by elevated temperature and organic pollutants. Aquat. Toxicol. 162, 82–93, http://dx.doi.org/10.1016/j.aquatox.2015.03.006.

Falfushynska, H., Gnatyshyna, L., Fedoruk, O., Sokolova, I.M., Stoliar, O., 2016. Endocrine activities and cellular stress responses in the marsh frog *Pelophylax ridibundus* exposed to cobalt, zinc and their organic nanocomplexes. Aquat. Toxicol. 170, 62–71, http://dx.doi.org/10.1016/j.aquatox.2015.11.006.

Frankenfeld, T.G., Correa Da Costa, V.M., Nascimento-Saba, C.C., Ortiga-Carvalho, T.M., Santos, R.M., Lisboa, P.C., Carvalho, D.P., Rosenthal, D., 2002. Thyroid and pituitary thyroxine-5'-deiodinase activity and thyrotrophin secretion in lithium-treated rats. J. Endocrinol. 174, 331–334, http://dx.doi.org/10.1677/joe.0.1740331.

Franklin, R.B., Costello, L.C., 2009. The important role of the apoptotic effects of zinc in the development of cancers. J. Cell Biochem. 106, 750–757, http://dx.doi.org/10.1002/jcb.22049.

Gagné, F., Turcotte, P., Auclair, J., Gagnon, C., 2013. The effects of zinc oxide nanoparticles on the metallome in freshwater mussels. Comp. Biochem. Physiol. 158C, 22–28, http://dx.doi.org/10.1016/j.cbpc.2013.04.001.

González Pondal, M., Paier, B., Noli, M.I., Tudino, M.B., Stripeikis, J.D., Hagmüller, K., Zaninovich, A.A., 1995. Changes induced by zinc on thyroxine deiodination by rat liver in vivo and in vitro. Acta Physiol. Pharmacol. Ther. Latinoam. 45, 35–41.

Goulet, F., Hélie, P., Vachon, P., 2010. Eugenol anesthesia in African clawed frogs (*Xenopus laevis*) of different body weights. J. Am. Assoc. Lab. Anim. Sci. 49, 460–463.

Griffith, O.W., 1980. Determination of glutathione and glutathione disulfide using glutathione reductase and 2-vinylpyridine. Anal. Biochem. 106, 207–212.

Hayes, T.B., Case, P., Chui, S., Chung, D., Haeffele, C., Haston, K., Lee, M., Mai, V.P., Marjuoa, Y., Parker, J., Tsui, M., 2006. Pesticide mixtures, endocrine disruption, and amphibian declines: are we underestimating the impact? Environ. Health Perspect. 114, 40–50, http://dx.doi.org/10.1289/ehp.8051.

Heberer, T., 2002. Occurrence, fate, and removal of pharmaceutical residues in the aquatic environment: a review of recent research data. Toxicol. Lett. 131, 5–17.

Hermes-Lima, M., Storey, K.B., 1998. Role of antioxidant defences in the tolerance of severe dehydration by anurans. The case of the leopard frog *Rana pipiens*. Mol. Cell. Biochem. 189, 79–89, http://dx.doi.org/10.1023/A:1006868208476.

Hinkle, P.M., Kinsella, P.A., Osterhoudt, K.C., 1987. Cadmium uptake and toxicity via voltage-sensitive calcium channels. J. Biol. Chem. 262, 16333–16337, http://dx.doi.org/10.1006/taap.1994.1012.

Hoffmann, F., Kloas, W., 2012. Estrogens can disrupt amphibian mating behavior. PLoS One 7, e32097, http://dx.doi.org/10.1371/journal.pone.0032097.

Huang, C.C., Aronstam, R.S., Chen, D.R., Huang, Y.W., 2010. Oxidative stress, calcium homeostasis, and altered gene expression in human lung epithelial cells exposed to ZnO nanoparticles. Toxicol. In Vitro. 24, 45–55, http://dx.doi.org/10.1016/j.tiv.2009.09.007.

Isani, G., Carpenè, E., 2014. Metallothioneins, unconventional proteins from unconventional animals: a long journey from nematodes to mammals. Biomolecules 2014, 435–457.

Kagi, J.H.R., Schaffer, A., 1988. Biochemistry of metallothionein. Biochemistry 27, 8509–8515.

Kang, Y.J., 2006. Metallothionein redox cycle and function. Exp. Biol. Med. 231, 1459–1467.

Kaya, H., Aydın, F., Gürkan, M., Yılmaz, S., Ates, M., Demir, V., Arslan, Z., 2015. Effects of zinc oxide nanoparticles on bioaccumulation and oxidative stress in

different organs of tilapia (*Oreochromis niloticus*). Environ. Toxicol. Pharmacol. 40, 936–947, http://dx.doi.org/10.1016/j.etap.2015.10.001.
Kikuchi, Y., Irie, M., Ikebuchi, H., Sawada, J., Terao, T., Nakayama, S., Iguchi, S., Okada, Y., 1990. Antigenic determinants on rat metallothionein: fine epitope mapping for a murine monoclonal antibody and rabbit polyclonal antisera. J. Biochem. 107, 650–654.
Kloas, W., Urbatzka, R., Opitz, R., Würtz, S., Behrends, T., Hermelink, B., Hofmann, F., Jagnytsch, O., Kroupova, H., Lorenz, C., Neumann, N., Pietsch, C., Trubiroha, A., Van Ballegooy, C., Wiedemann, C., Lutz, I., 2009. Endocrine disruption in aquatic vertebrates. Ann. N.Y. Acad. Sci. 1163, 187–200, http://dx.doi.org/10.1111/j.1749-6632.2009.04453.x.
Kolpin, D.W., Furlong, E.T., Meyer, M.T., Thurman, E.M., Zaugg, S.D., Barber, L.B., Buxton, H.T., 2002. Pharmaceuticals, hormones, and other organic wastewater contaminants in U. S. streams: 1999–2000: a national reconnaissance. Environ. Sci. Technol. 36, 1202–1211.
Kondo, S., Yin, D., Morimura, T., Kubo, H., Nakatsu, S., Takeuchi, J., 1995. Combination therapy with cisplatin and nifedipine induces apoptosis in cisplatin-sensitive and cisplatin-resistant human glioblastoma cells. Br. J. Cancer 71, 282–289, http://dx.doi.org/10.1038/bjc.1995.57.
Leslie, E.M., Liu, J., Klaassen, C.D., Waalkes, M.P., 2006. Acquired cadmium resistance in metallothionein-i/ii (−/−) knockout cells: role of the T-type calcium channel cacnα1G in cadmium uptake. Mol. Pharmacol. 69, 2629–2639.
Li, Z., Zhang, S., Liu, Q., 2008. Vitellogenin functions as a multivalent pattern recognition receptor with an opsonic activity. PLoS One 3, e1940, http://dx.doi.org/10.1371/journal.pone.0001940.
Li, N., Ma, M., Rao, K., Wang, Z., 2011. In vitro thyroid disrupting effects of organic extracts from WWTPs in Beijing. J. Environ. Sci. (China) 23, 671–675, http://dx.doi.org/10.1016/S1001-0742(10)60461-5.
Lowry, O.H., Rosebrough, H.J., Farr, A.L., Randall, R.J., 1951. Protein measurement with the Folin phenol reagent. J. Biol. Chem. 193, 265–275.
Ludwiczek, S., Theurl, I., Muckenthaler, M.U., Jakab, M., Mair, S.M., Theur, L.M., Kiss, J., Paulmichl, M., Hentze, M.W., Ritter, M., Weiss, G., 2007. Ca2+ channel blockers reverse iron overload by a new mechanism via divalent metal transporter-1. Nat. Med. 13, 448–454, http://dx.doi.org/10.1038/nm1542.
MacDonald, R.S., 2000. The role of zinc in growth and cell proliferation. J. Nutr. 130, 1500S–1508S.
Manibabu, P.V., Patnaik, B.K., 1997. Lipofuscin concentration of the brain shows a reduction with age in male garden lizard. Comp. Biochem. Physiol. 117C, 229–232.
Manke, A., Wang, L., Rojanasakul, Y., 2013. 2013: Mechanisms of nanoparticle-induced oxidative stress and toxicity. Biomed. Res. Int 942916, http://dx.doi.org/10.1155/2013/942916.
Montorzi, M., Falchuk, K.H., Vallee, B.L., 1995. Vitellogenin and lipovitellin: zinc proteins of *Xenopus laevis* oocytes. Biochemistry 34, 10851–10858, http://dx.doi.org/10.1021/bi00034a018.
Narayan, E.J., 2013. Non-invasive reproductive and stress endocrinology in amphibian conservation physiology. Conserv. Physiol. 1, cot011, http://dx.doi.org/10.1093/conphys/cot011.
Nations, S., Wages, M., Cañas, J.E., Maul, J., Theodorakis, C., Cobb, G.P., 2011. Acute effects of Fe2O3, TiO2, ZnO and CuO nanomaterials on *Xenopus laevi*. Chemosphere 83, 1053–1061, http://dx.doi.org/10.1016/j.chemosphere.2011.01.061.
Ngu, T.T., Stillman, M.J., 2009. Metalation of metallothioneins. IUBMB Life 61, 438–446, http://dx.doi.org/10.1002/iub.182.
Nielson, K.B., Winge, D.R., 1985. Independence of the domains of metallothionein in metal binding. J. Biol. Chem. 260, 8698–8701.
Ohkawa, H., Onishi, N., Yagi, K., 1979. Assay for lipid peroxidation in animal tissue by thiobarbituric acid reaction. Anal. Biochem. 95, 351–358.
Olive, P.L., 1988. DNA precipitation assay: a rapid and simple method for detecting DNA damage in mammalian cells. Environ. Mol. Mutagen. 11, 487–495.
Palmer, B.D., Huth, L.K., Pieto, D.L., Selcer, K.W., 1998. Vitellogenin as a biomarker for xenobiotic estrogens in an amphibian model system. Environ. Toxicol. Chem. 17, 30–36, http://dx.doi.org/10.1002/etc.5620170105.
Papatsonis, D.N., Bos, J.M., van Geijn, H.P., Lok, C.A., Dekker, G.A., 2007. Nifedipine pharmacokinetics and plasma levels in the management of preterm labor. Am. J. Ther. 14, 346–350, http://dx.doi.org/10.1021/es011055j.
Poteat, M.D., Díaz-Jaramillo, M., Buchwalter, D.B., 2012a. Divalent metal (Ca, Cd, Mn, Zn) uptake and interactions in the aquatic insect *Hydropsyche sparna*. J. Exp. Biol. 215, 1575–1583, http://dx.doi.org/10.1093/conphys/cot011.
Poteat, M.D., Díaz-Jaramillo, M., Buchwalter, D.B., 2012b. Divalent metal (Ca, Cd, Mn, Zn) uptake and interactions in the aquatic insect *Hydropsyche sparna*. J. Exp. Biol. 215, 1575–1583, http://dx.doi.org/10.1242/jeb.063412.
Ray, S., Mondal, S., Dana, N., 2012. Evaluation of protective role of nifedipine on lipid peroxidation using reduced glutathione as model marker. Oxid. Antioxid. Med. Sci. 1, 97–100, http://dx.doi.org/10.5455/oams.170812.or.012.
Rouhani Rankouhi, T., Sanderson, J.T., van Holsteijn, I., van Kooten, P., Bosveld, A.T.C., van den Berg, M., 2005. Effects of environmental and natural estrogens on vitellogenin production in hepatocytes of the brown frog (*Rana temporaria*). Aquat. Toxicol. 71, 97–101, http://dx.doi.org/10.1016/j.aquatox.2004.09.009.
Schaider, L.A., Ackerman, J.M., Rudel, R.A., 2016. Septic systems as sources of organic wastewater compounds in domestic drinking water wells in a shallow sand and gravel aquifer. Sci. Total Environ. 547, 470–481, http://dx.doi.org/10.1016/j.scitotenv.2015.12.081.
Shoae-Hagh, P., Rahimifard, M., Navaei-Nigjeh, M., Baeeri, M., Gholami, M., Mohammadirad, A., Abdollahi, M., 2014. Zinc oxide nanoparticles reduce apoptosis and oxidative stress values in isolated rat pancreatic islets. Biol. Trace Elem. Res. 162, 262–269, http://dx.doi.org/10.1007/s12011-014-0113-6.
Suzuki, K.T., Itoh, N., Ohta, K., Sunaga, H., 1986. Amphibian metallothionein. Induction in the frogs *Rana japonica*, *R. nigromaculata* and *Rhacophorus schlegelii*. Comp. Biochem. Physiol. 83C, 253–259.
Suzuki, K.T., 1991. Purification of vertebrate metallothioneins. Meth. Enzymol. 205, 252–263.
Tan, T.K., Khiew, P.S., Chiu, W.S., Radiman, S., Abd-Shukor, R., Huang, N.M., Lim, H.N., 2011. Photodegradation of phenol red in the presence of ZnO nanoparticles. Int. J. Chem. Mol. Nucl. Mater. Metallurg. Eng. 5, 613–618.
Thompson, E.D., Mayer, G.D., Glover, C.N., Capo, T., Walsh, P.J., Hogstrand, C., 2012. Zinc hyperaccumulation in squirrelfish (*Holocentrus adscenscionis*) and its role in embryo viability. PLoS One 7, e46127, http://dx.doi.org/10.1371/journal.pone.0046127.
Truong-Tran, A.Q., Carter, J., Ruffin, R.E., Zalewski, P.D., 2001. The role of zinc in caspase activation and apoptotic cell death. Biometals 14, 315–330, http://dx.doi.org/10.1023/A:1012993017026.
Unuma, T., Sawaguchi, S., Yamano, K., Ohta, H., 2011. Accumulation of the major yolk protein and zinc in the agametogenic sea urchin gonad. Biol. Bull. 221, 227–237.
Valko, M., Morris, H., Cronin, M.T., 2005. Metals toxicity and oxidative stress. Curr. Med. Chem. 12, 1161–1208, http://dx.doi.org/10.2174/0929867053764635.
Velena, A., Zarkovic, N., Gall Troselj, K., Bisenieks, E., Krauze, A., Poikans, J., Duburs, G., 2016. 1,4-Dihydropyridine derivatives: dihydronicotinamide analogues-Model compounds targeting oxidative stress. Oxid. Med. Cell. Longev. 189241, http://dx.doi.org/10.1155/2016/1892412.
Venturino, A., Rosenbaum, E., Caballero de Castro, A., Anguiano, O.L., Gauna, L., Fonovich de Schroeder, T., Pechen de D'Angelo, A.M., 2003. Biomarkers of effect in toads and frogs. Biomarkers 8, 167–186, http://dx.doi.org/10.1080/1354700031000120116.
Viarengo, A., Ponzano, E., Dondero, F., Fabbri, R., 1997. A simple spectrophotometric method for metallothionein evaluation in marine organisms: an application to Mediterranean and Antarctic Molluscs. Mar. Environ. Res. 44, 69–84.
Viarengo, A., Burlando, B., Cavaletto, M., Marchi, B., Ponzano, E., Blasco, J., 1999. Role of metallothionein against oxidative stress in the mussel *Mytilus galloprovincialis*. Am. J. Physiol. 277, R1612–1619.
Wang, L.P., Jiang, Y., Yang, H., Peng, C., Zhang, C., Tao, X., Xie, H.H., 2016. Combination therapy of nifedipine and sulphonylureas exhibits a mutual antagonistic effect on the endothelial cell dysfunction induced by hyperglycemia linked to vascular disease. Cell. Physiol. Biochem. 38, 2337–2347, http://dx.doi.org/10.1159/000445587.
Whittaker, K., Koo, M.S., Wake, D.B., Vredenburg, V.T., 2013. Global declines of amphibians. In: Levin, S.A. (Ed.), Encyclopedia of Biodiversity, 3, second edition, pp. 691–699.
Wong, S.W., Leung, P.T., Djurisić, A.B., Leung, K.M., 2010. Toxicities of nano zinc oxide to five marine organisms: influences of aggregate size and ion solubility. Anal. Bioanal. Chem. 396, 609–618, http://dx.doi.org/10.1007/s00216-009-3249-z.
Yang, X., Shao, H., Liu, W., Gu, W., Shu, X., Mo, Y., Chen, X., Zhang, Q., Jiang, M., 2015. Endoplasmic reticulum stress and oxidative stress are involved in ZnO nanoparticle-induced hepatotoxicity. Toxicol. Lett. 234, 40–49, http://dx.doi.org/10.1016/j.toxlet.2015.02.004.
Zhang, J., Wages, M., Cox, S.B., Maul, J.D., Li, Y., Barnes, M., Hope-Weeks, L., Cobb, G.P., 2012. Effect of titanium dioxide nanomaterials and ultraviolet light coexposure on African Clawed Frogs textit (*Xenopus laevis*). Ecotoxicol. Environ. Saf. 31, 176–183, http://dx.doi.org/10.1002/etc.718.
Zhao, C.Y., Tan, S.X., Xiao, X.Y., Qiu, X.S., Pan, J.Q., Tang, Z.X., 2014. Effects of dietary zinc oxide nanoparticles on growth performance and antioxidative status in broilers. Biol. Trace Elem. Res. 160, 361–367, http://dx.doi.org/10.1007/s12011-014-0052-2.